Evidence of unique-parity band structure in neutron-rich odd-A Ru isotopes

K. Butler-Moore, R. Aryaeinejad, J. D. Cole, Y. Dardenne, and R. G. Greenwood
Idaho National Engineering Laboratory, Idaho Falls, Idaho 83415

J. H. Hamilton, A. V. Ramayya, W.-C. Ma, and B. R. S. Babu
Physics Department, Vanderbilt University, Nashville, Tennessee 37235

J. O. Rasmussen, M. A. Stoyer, S. Y. Chu, K. E. Gregorich, M. Mohar, and S. Asztalus
Lawrence Berkeley Laboratory, Berkeley, California 94720

S. G. Prussin
Nuclear Engineering Department, University of California–Berkeley, Berkeley, California 94720

K. J. Moody, R. W. Lougheed, and J. F. Wild
Lawrence Livermore National Laboratory, Livermore, California 94550
(Received 20 January 1995)

With prompt γ-ray and x-ray spectroscopy on fission fragments, several new transitions in ^{109,111}Ru have been identified. Angular correlation analysis of several of the new transitions yield evidence of a stretched $E2$ band structure. Qualitative Nilsson model arguments, systematics, and triaxial rotor+particle calculations support our hypothesis that the observed band is built on the unique parity $\nu h_{11/2}$ orbital.

PACS number(s): 21.10.Re, 23.20.Lv, 27.60.+j, 27.70.+q

I. INTRODUCTION

The fission process produces several hundred neutron-rich nuclides, many of which can be produced by no other means. The spontaneously fissioning (SF) isotope ^{252}Cf is one that many nuclear spectroscopists have chosen to produce neutron-rich fragments. Of particular importance in *prompt* γ-ray spectroscopy is the fact that ^{252}Cf has one of the best fission to alpha decay ratios, which means far fewer contaminant peaks need be dealt with in data analysis. Despite the advantages of a ^{252}Cf source, the tremendous number of transitions involved makes data analysis difficult. After the pioneering coincidence studies of the early 1970s [1], in which many $2^+ \rightarrow 0^+$ and $4^+ \rightarrow 2^+$ transitions of even-even neutron-rich nuclei were discovered, there was a hiatus in prompt spectroscopy of fission fragments.

The recent use of SF sources in Compton-suppressed Ge detector arrays has produced huge data sets that are much cleaner than in the early studies. As a result, prompt spectroscopists have revealed such interesting nuclear phenomena as octupole bands in heavy Ce and Ba nuclides [2], and the structure of nuclides near double magic ^{132}Sn [3]. Many fission fragments with $A \sim 110$ are known to be transitional, and some exhibit features of triaxial nuclei. In a previous paper [4], discoveries via prompt γ-ray spectroscopy on ^{252}Cf fission fragments allowed us to extend the backbending systematics in even Pd isotopes to the neutron-rich nuclides ^{122,114,116}Pd. In this paper, we continue our SF prompt spectroscopy in the $A \sim 110$ region by presenting the nuclear structure of two odd-A neutron-rich Ru nuclides, ^{109,111}Ru.

The paper is organized as follows: In Sec. II a brief description of the experimental apparatus used to take coincidence data is given, and in Sec. III we explain how the data are analyzed. Several spectra that support our level scheme assignments for ^{109,111}Ru are presented in Sec. IV. In Sec. V spins and parities are assigned to states based upon experimental measurements and systematics. The results of these studies suggest, for each nuclide ^{109,111}Ru, the existence of a band of states arising from the coupling of an $h_{11/2}$ neutron to an even-even core. Assuming this observation is true, in Sec. VI we perform particle+triaxial core calculations for ^{109,111}Ru.

II. EXPERIMENTAL SETUPS

The data presented in this paper result from two different coincidence experiments: (1) the 36 Ge detector array of the early implementation of GAMMASPHERE and (2) a three Ge and two low-energy photon spectroscopic (LEPS) x-ray detector system at the INEL.

In both experiments a spontaneous fission source of ^{252}Cf, with a strength of about 6×10^4 fissions per second (0.1 μg), was used. The source for the GAMMASPHERE experiment was sandwiched between Ni and thin Al backing. The INEL source was designed with a 250 μm Be window, so that x rays would not be attenuated significantly.

The early implementation of GAMMASPHERE (Fall 1993) consisted of 36 80% Ge detectors, and one LEPS x-ray detector. Each Ge detector is Compton suppressed with BGO shields, and on average has a resolution of about 2.5 keV at 1332 keV. The distance of the Ge detectors from the source was 25–30 cm. The experiment was carried out for a period of 2 weeks. An event was recorded to tape when at least two γ rays were detected within a timing coincidence gate of 100 ns. Approximately 110 Gbytes of data were taken; about 30% of the data consists of triple coincidences. A γ-γ-γ cube and nine γ-γ coincidence matrices (one for each angle

in the angular correlation measurements) were built from the raw events.

Even though the GAMMASPHERE x-ray detector did not have a BGO shield, x-ray production in and scattering of photons from BGO shields of the suppressed Ge detectors adversely affected the quality of the x-ray data. Data of better quality were obtained with a less complicated INEL apparatus.

The INEL experimental setup consisted of three 25% n-type Ge detectors and two 2.5-cm^3 LEPS detectors operating in coincidence mode. The energy resolution for the Ge detectors was 2.1 keV at 1332 keV and, for the LEPS detectors, 280 eV at 14 keV. The source-to-detector distances were 2.5 cm for the LEPS detectors and 9 cm for all Ge detectors. None of the Ge or x-ray detectors were Compton suppressed. The lack of suppression had an adverse effect on the quality of γ-ray data, but the x-ray data were relatively enhanced, as there was much less scattering.

The INEL experiment ran continuously for about 4 months, during which about 1.3×10^{10} double coincidence events were collected. The hardware master gate was triggered by coincidences between two x-rays or one x-ray and one γ-ray detector. Two $4K\times4K$ matrices for x-x and x-γ coincidences were generated by requiring the timing coincidence gate to be 50 ns wide.

The structure of odd-A nuclei usually consists of several γ-ray transitions so low in energy that they are detected poorly, if at all, by standard Ge detectors. Several low-energy γ-ray transitions that were absolutely essential in unraveling the structure of the neutron-rich nuclides ^{109,111}Ru could not have been detected without LEPS detectors.

III. DATA ANALYSIS AND TECHNIQUES

A. Physical principles

Underlying the principal technique used in prompt γ-ray spectroscopy of fission fragments is a basic concept: Z and A conservation. With these conservation rules, and a knowledge of the time scale of fragment deexcitation (from initial formation to stable nuclide), one can unravel decay schemes consisting of many γ rays.

Upon scission of ^{252}Cf, two neutron-rich fragments are produced. (Very rarely, there might be a fragmentation involving three pieces.) Evaporation of about four neutrons (shared between the two fragments) follows within femtoseconds. Each fragment then deexcites by prompt γ-ray emission, which usually occurs in a time span of a 0.001–100 ns. Following prompt γ-ray deexcitation to the ground state, the neutron-rich nuclide β^- decays to a daughter nuclide which is nearer the line of stability. The β-decay process typically takes from milliseconds to hours or days.

If a suitable gate, say, 100 ns, is set as the timing coincidence gate, neutron emission and prompt γ-ray deexcitation are defined as simultaneous within the logic of the coincidence detector system. The same timing gate will also register coincident transitions between states populated by β^- decay. Fortunately, prompt γ rays can be distinguished from those populated by β^- decay by utilizing proton and nucleon number conservation. While a given nuclide Z is deexciting by prompt γ-ray emission, simultaneously its partner fragment $\bar{Z}$ ($\bar{Z}=98-Z$) will be emitting prompt γ rays. There are many channels for fission decay—one to five neutron emissions per fission is very likely for the spontaneous fission of ^{252}Cf. Now consider an energy gate on a E_γ-E_γ coincidence matrix that corresponds to a transition in the nuclide Z. Then the signature of a prompt component to the transition is the appearance of transitions from *several* different nuclides, all with the same complementary atomic number $\bar{Z}(=98-Z)$.

Prompt γ rays are also in coincidence with x rays because of the competition between internal conversion and γ-ray emission. Transitions low in energy are more effectively converted than transitions higher in energy, and the nuclear structure of many odd-A and odd-odd nuclei typically consists of many transitions in the range of 50–200 keV. Therefore, a large proportion of the $K\alpha$ line corresponding to fragments with atomic number Z is due to internal conversions among the odd-A and odd-odd nuclei.

B. Data structures

Matrices of x-x, x-γ, and γ-γ coincidences were built and analyzed with software available from Oak Ridge National Laboratory. A spectrum generated by gating a γ-γ matrix often has numerous "spurious" peaks. These peaks usually arise because the gate overlaps prominent transitions in several different nuclides. After all, there are about 100 nuclides with significant fission yields represented in the coincidence matrix. The triple coincidence technique can yield spectra that are much more free of spurious peaks. Our triple coincidence "cube" was built and analyzed with software available from Chalk River Laboratory.

As is evident from recent publications on fission fragment spectroscopy [3–6], triplet coincidence analysis is becoming an indispensable tool for these types of structure studies. Many of the new transitions in ^{109,111}Ru are much more easily discerned in the γ-γ-γ data. Two-dimensional data structures were used for placement of low-energy γ rays and for the measurement of angular correlation (AC) between successive γ-ray transitions.

C. Angular correlation matrices

Typically, angular correlation experiments are performed by varying the angle of one detector with respect to a fixed detector. For the GAMMASPHERE data on which we performed our AC measurements, the choice of angles is constrained by the known geometry of the 36-detector array. Between each pair of the 630 possible pairs, an AC angle θ is defined by rays that start at the Cf source and penetrate the midpoint of the face of each detector. Since the applicable angular distribution formula

$$W(\theta)=\text{const}[1+a_2P_2(\cos\theta)+a_4P_4(\cos\theta)] \quad (1)$$

depends only on even powers of $\cos\theta$, and because of the high degree of symmetry in the detector array, many distinct pairs of detectors may contribute to a given AC angle θ.

In order to simplify analysis by limiting the number of γ-γ matrices created, only coincidences from detectors that were nearly equivalent in efficiency were considered. This was the only criterion for our "identical detector approxima-

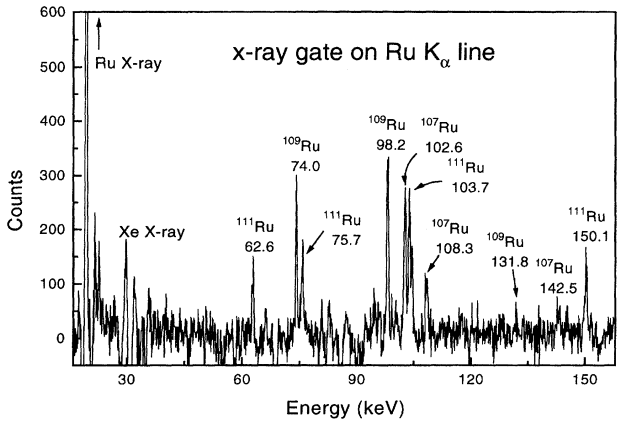

FIG. 1. X-Ray gate on Ru $K\alpha$ line from INEL LEPS detectors. Besides the strong Ru x-ray and the complementary Xe x-ray lines, many low-energy γ rays of odd Ru isotopes can be detected.

tion," and, of course, neglects other factors such as small differences in solid angle correction factors among the different detectors. Nine AC angles between 90° and 180° were chosen. Angles chosen were those that had a large number of contributing pairs of detectors within an angle bin of about $\pm 1°$. Since some AC angles are represented by more detector pairs than others, appropriate scaling factors were used to scale peak intensities.

The directional correlation of several strong transitions of known multipolarity was analyzed via the matrices created by the forgoing procedure. Preliminary analysis indicated that the peak areas corresponding to only one AC angle (136°) systematically deviated from the expected smooth trend observed with the other AC angles. Rather than eliminate this data point, which could probably be justified since only seven detector pairs contributed to this AC angle, a small correction factor was applied to bring it more in line.

Several correction procedures typical in high-precision AC experiments were not performed. We did not correct for accidental coincidences or for the angular dependence of the solid angle correction factors. Confidence in our identical detector approximation and the neglect of the corrections was gained by the analysis of several cascades of γ rays from high-yield fission fragments. The results of this preliminary analysis were consistent with theoretical expectations. Later, examples of AC data will be presented for cascades in ^{109,111}Ru.

IV. IDENTIFICATION OF γ-RAY TRANSITIONS

The first step in the creation of level schemes for ^{109,111}Ru was to examine the γ rays in coincidence with Ru x rays. Figure 1 shows the spectrum that results from gating on the Ru $K\alpha$ line. A notable advantage of a gate involving x-ray detectors is the possibility of observing low-energy γ rays. Identity assignment for the major peaks in Fig. 1 have relied on previous studies, as cited in the Online National Nuclear Data Center (Brookhaven). The β^- decay work of Penttilä [7] has also proved to be a valuable source of information for the low-lying states of ^{109}Ru.

It is convenient to partition the structure of the Ru nuclides, depicted in Fig. 2, into low- and high-energy regions. In this classification, high-energy states have an excitation energy above 600 keV. Spectra and arguments that support the assignment of the low-energy structure of ^{109,111}Ru nuclides are now considered.

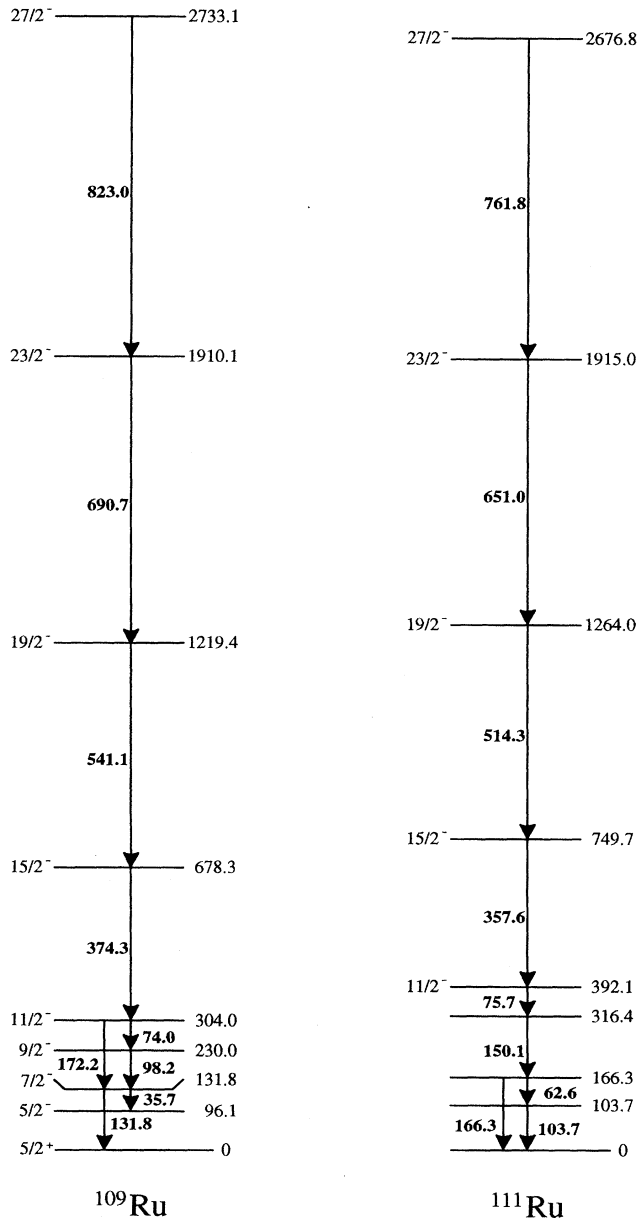

FIG. 2. Level schemes of ^{109}Ru and ^{111}Ru, with emphasis on the apparent band structure populated in the spontaneous fission process. Spin assignments for ^{109}Ru are based on directional correlation and conversion electron measurements. Spin assignments for ^{111}Ru are based on systematics. State energies are labeled in keV. The known 96.1-keV transition in ^{109}Ru is not shown because it is not observed in prompt coincidence ($T_{1/2}$=540 ns) [7].

A. Low-lying excited states

From previous SF studies [8], the prompt nuclear structure of ^{111}Ru had been identified up to the state with energy

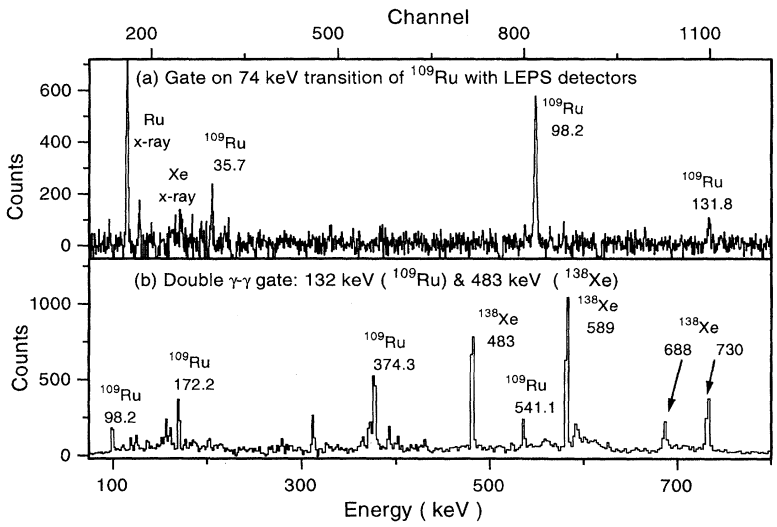

FIG. 3. Spectra to confirm lower-energy portion of decay scheme of ^{109}Ru. (a) Gate on 74-keV transition of ^{109}Ru with LEPS detectors. (b) Double γ-γ gate on 132-keV transition of ^{109}Ru and the 483-keV doublet in ^{138}Xe. This and all following spectra are from GAMMASPHERE data.

749.7 keV. Except for differences of at most 0.4 keV in transition energies, our work corroborates this. The same reference presents a level scheme for ^{109}Ru, but it is partially incorrect. Although the transitions of 98.2, 74.0, 172.2, and 374.3 keV are placed in the correct *relative* order, the cascade is not correctly connected with the ground state. The problem lies with the 131.8-keV transition, which was placed by Hopkins *et al.* as feeding the 74.0-keV transition. The resolution of this (quite understandable) mistake relies on careful β^- decay studies of ^{109}Ru.

A state that decays to the ground state via a 131.8-keV transition is reported by Penttilä [7]. He also reports a 98.2-keV transition that feeds the 131.8-keV state, and we assert that this is the same one we see in our prompt spectroscopy data. There are two possibilities as to why the 131.8-keV transition was misplaced by Hopkins *et al.* (1) If a state has a lifetime longer than the timing coincidence gate, the transition from that state will be attenuated in intensity. Many of the low-lying states in ^{109}Ru have appreciable lifetimes. The 96.1-keV state has a lifetime of 540 ns. There also exists a 68.8-keV state that decays to the ground state with a lifetime of 500 ns. Neither of these states' decays to the ground state were observed in our prompt spectroscopy work, and so they are not shown in Fig. 2. (2) If the 131.8-keV transition is a crossover transition, its γ-ray strength would appear attenuated relative to transitions higher in the band structure. Since it is customary to use peak intensity arguments to place transitions in the proper relative positions, either attenuation mechanism could have led to the misplacement of the 131.8-keV transition.

The x-ray and low-energy γ-ray spectra that result from a gate on the 74.0-keV transition as detected by our LEPS detectors are shown in Fig. 3(a). The transitions marked are consistent with our level scheme of ^{109}Ru. The relatively weak intensity of the 131.8-keV transition is easily observed. Convincing evidence that the 131.8-keV transition connects the known sequence of transitions with the ground state is shown in Fig. 3(b). This figure was generated by double gating GAMMASPHERE data on transitions of energy 131.8 keV and 483 keV. The 483-keV gate was chosen because it is known [3] that there exist two, strong consecutive transitions of about 483 keV in ^{138}Xe. ^{138}Xe transitions will be in coincidence with those of ^{109}Ru because ^{138}Xe is the five-neutron complement to ^{109}Ru. Known ^{138}Xe peaks have been indicated in Fig. 4(b). Despite the very low efficiency of the Ge detector array at 100 keV, the 98.2-keV transition is clearly seen. Also present are the 172.2-, 374.3-, and 541.1-keV transitions in ^{109}Ru.

B. High-lying excited states

The 374.3- and 541.1-keV pair of transitions noted in Fig. 3(b) was initially discovered with x-γ and γ-γ spectra analysis. Since they are readily observed in Fig. 3(b), we do not present another spectrum here. Since both the 374.3- and 541.1-keV transitions lie above low-energy γ-ray detection threshold, this pair of transitions in ^{109}Ru makes an excellent candidate for a double gated spectrum with our high-statistics GAMMASPHERE data. The resulting triple coincidence spectrum is shown in Fig. 4(a). Peaks corresponding to complementary Xe transitions have been marked, along with an easily identifiable 690.7-keV transition. Numerous double gates involving the 823.0-keV transition and transitions lower in the level scheme confirm its placement in ^{109}Ru.

The level scheme of ^{111}Ru was built in a manner similar to that of ^{109}Ru. Since our work on the states below 600 keV agrees with that of Hopkins *et al.* [8], we do not display spectra to confirm these results. A LEPS gate on the 75.7-keV transition in ^{111}Ru presented two candidate transitions, 357.6 and 514.3 keV, for triples analysis. The resulting double gated spectrum appears as Fig. 4(b). The 651.0- and 761.8-keV transitions are assigned to the ^{111}Ry yrast cascade. As in ^{109}Ru, numerous spectra were examined to confirm these results.

V. SPIN AND PARITY ASSIGNMENTS

The transitions between high-lying states in ^{109,111}Ru are monotonically increasing in energy. Naturally, a band structure of common origin is suspected for both. The experimental evidence for a negative-parity band structure will rely on

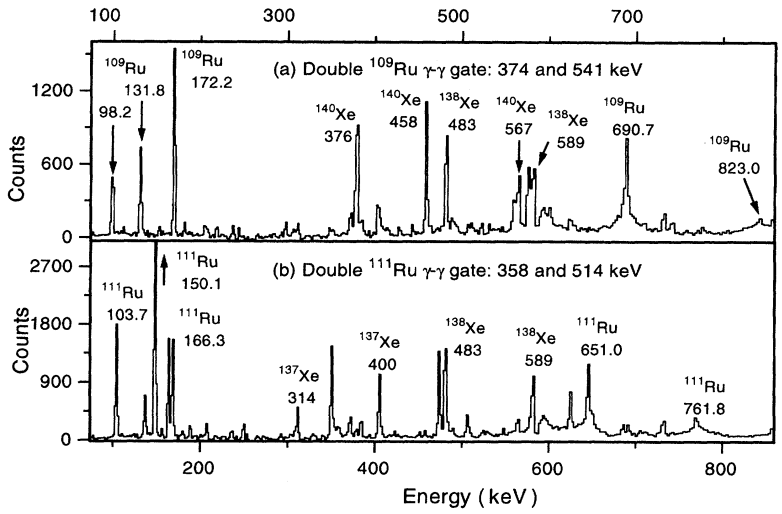

FIG. 4. Spectra to confirm higher-energy portion of decay schemes. (a) Triplet coincidence spectrum formed from the 374- and 541-keV transitions of ^{109}Ru. (b) Triple coincidence spectrum generated from the 358- and 514-keV γ rays of ^{111}Ru.

multipolarity assignments based on previous conversion electron work [7] and on our own AC work. Systematics and Nilsson model considerations also lend credibility to our spin and parity assignments.

A. Angular correlation and conversion electron measurements

Gamma-ray angular correlation (without polarization) discloses only the order of a multipole transition, and not its electric or magnetic character. Despite this limitation, AC measurements reveal that the high-energy transitions are quadrupole, which is consistent with the hypothesis of stretched $E2$ transitions. Figures 5(a), 6(a), and 6(b) are illustrative examples of the data for high-energy transitions in ^{109,111}Ru. Least-squares fitting of these data with the theoretical formula (1) permits extraction of the a_2 and a_4 values, which are consistent with the theoretical predictions for a quadrupole-quadrupole cascade. The results of AC analysis on low-energy as well as high-energy transitions appear in Table I.

Some of the low-energy cascades proceed through an unobserved intermediary γ-ray transition, which is placed in parentheses. The unobserved transition gives rise to some deorientation of the radiation oriented by the observation of the first member of the cascade. Though the amplitude of the resulting angular correlation should be decreased, in the cases analyzed, the dipole character is easily ascertained by negative values for the a_2 coefficient. Two examples of dipole directional correlations appear in Fig. 5(c) and Fig. 6(c).

Our AC measurements on cascades of ^{109}Ru are consistent with the conversion electron work of Penttilä [7]. Multipolarity, or, when these are not available, our AC results for γ-ray transitions in ^{109}Ru, are shown in Fig. 7. Together, they allow essentially unique spin and parity assignments for ^{109}Ru, if a ground state spin of $5/2^+$ is assumed. This ground state spin assignment is supported by β-decay properties of ^{109}Ru.

The 131.8-keV $E1$ transition to the (assumed) $5/2^+$ ground state compels the 131.8-keV state to be $3/2^-$, $5/2^-$, or $7/2^-$. Assume this state to have $J^\pi = 3/2^-$ or $5/2^-$. Then the 172.2-keV quadrupole transition feeding the 131.8-keV state forces the 304.0-keV state to have J^π from 1/2 to 9/2. Now the ground state of ^{109}Tc, which β decays to ^{109}Ru, is expected to be $7/2^+$. The spin of states predicted from allowed β decays of ^{109}Tc to ^{109}Ru would be 9/2 and less.

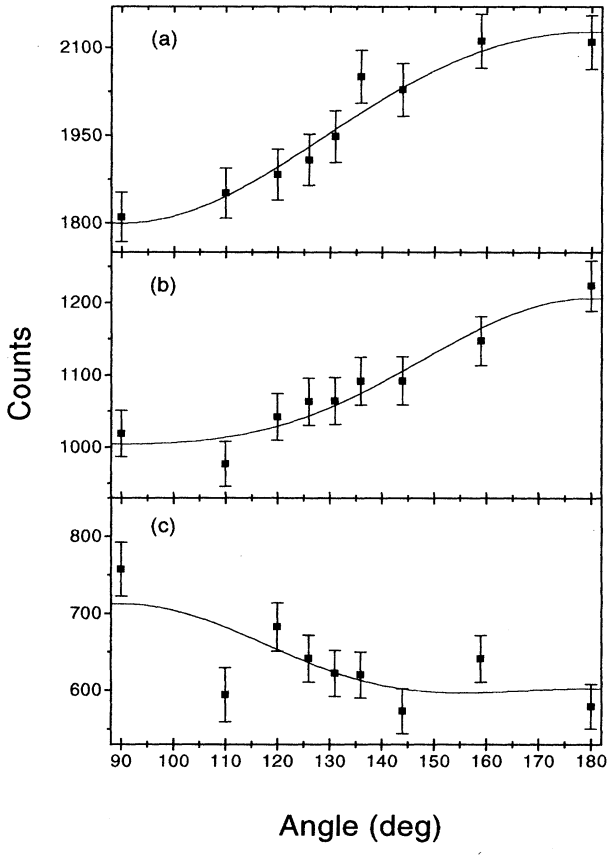

FIG. 5. Directional correlations of γ-ray cascades in ^{109}Ru. Curves correspond to the best fit of data to angular distribution formula; a_2 and a_4 results are in Table I. (a) 541 keV→374 keV cascade. (b) 374 keV→172 keV cascade. (c) 172 keV→132 keV cascade.

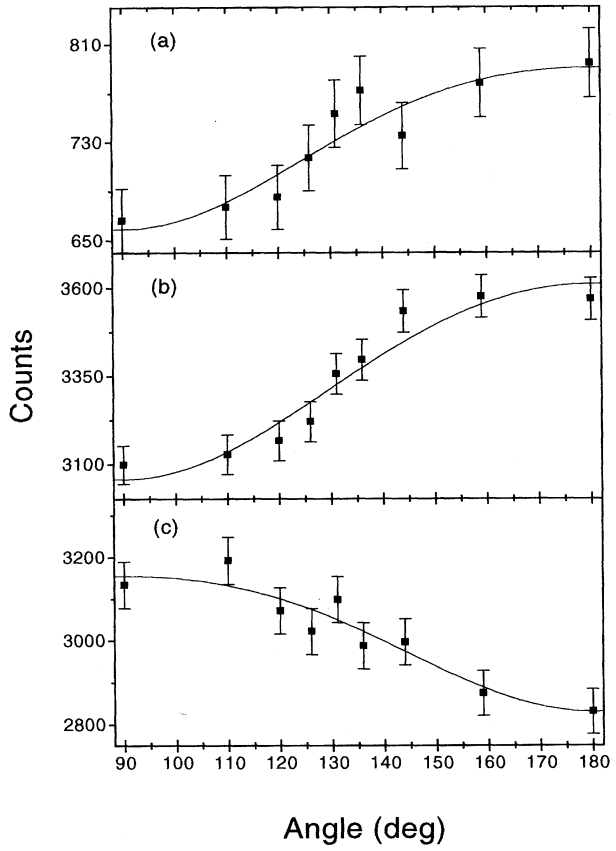

FIG. 6. Directional correlations of γ-ray cascades in ^{111}Ru. Curves correspond to best fit of data to angular distribution formula; a_2 and a_4 results are in Table I. (a) 651 keV→514 keV cascade. (b) 514 keV→358 keV cascade. (b) 358 keV→(76 keV)→132 keV cascade. The 76-keV transition is an intermediate, unobserved transition.

However, the 304.0-keV state has not been observed in extensive β-decay work, which implies that this state has spin greater than 9/2. On this basis, the 131.8-keV state is assigned $J^\pi = 7/2^-$ and the 304.0-keV state a spin of 11/2.

The experimental values of a_2 in Table I also allow elimination of certain spins for the 131.8-keV state. The positive value of a_2 near 0.1 implies that the 172.2-keV transition is quadrupole in character. Suppose $J^\pi = 5/2^-$ for the 131.8-keV state. Then the 304.0-keV state must have $J^\pi = 9/2^-$. This implies that the 172→132 keV cascade would be 9/2 (2) 5/2 (1) 5/2. However, the theoretical a_2 value for such a cascade is *positive*, in disagreement with the *negative* extracted value of -0.14 ± 0.04. In this way, the $J^\pi = 5/2^-$ possibility for the 131.8-keV state can be eliminated. The experimental a_2 value has the same sign as the theoretical a_2 value for a 11/2 (2) 7/2 (1) 5/2 cascade.

The $M1$ transition between the $J^\pi = 7/2^-$ state and the state at 96.1 keV and the $E1$ transition between this state and the ground state imply that the 96.1-keV state must have $J^\pi = 5/2^-$. The last low-energy state to be considered has an excitation energy of 230.0 keV. The $M1$ transition between it and the $J^\pi = 7/2^-$ state compels it to have $J^\pi = 9/2^-$.

B. Odd-*A* systematics for $N \sim 65$

The assignments made thus far agree with simple Nilsson model considerations and systematics. The Ru isotopes near $A \sim 110$ have rather large deformations and axial asymmetry ($\beta \sim 0.3$ and $\gamma \sim 24°$) [9]. Though the precise positions of Nilsson orbits depends sensitively on β and γ, from an ordinary Nilsson diagram [10], it is seen that the 65th neutron will most likely fill the $5/2^+[413]$ state (at $\beta = 0$, the $g_{7/2}$ spherical orbital) or the unique-parity state $5/2^-[532]$ (at $\beta = 0$, the $h_{11/2}$ spherical orbital). The $g_{7/2}$ orbit is strongly mixed with the $d_{5/2}$ configuration.

The $5/2^+$ ground state assumption for ^{109}Ru is consistent with it being the bandhead of the $5/2^+[413]$ Nilsson orbital. In fact, many odd-A Pd and Cd isotopes near $A \sim 110$ have positive-parity band structures built on the $g_{7/2}$ orbital. However, most of the γ-ray strength in these neighbors of ^{109}Ru pass through a negative-parity band. For instance, in ^{107}Pd [11] the known yrast band consists of negative-parity states $J^\pi = 11/2^- - 39/2^-$, and contains about 90% of the known γ-ray transition strength. The nonobservance of positive-parity band structures in ^{109}Ru is due to the fact that the SF process predominantly populates the yrast band. The

TABLE I. Directional distribution coefficients in ^{109,111}Ru.

Nuclide	Cascade $\gamma_1 \rightarrow \gamma_2$	a_2	a_4	Multiple order of γ_2
^{109}Ru	691→541	0.19±0.05	−0.05±0.05	Q[a]
	541→374	0.12±0.02	−0.01±0.02	Q
	374→172	0.12±0.03	0.03±0.03	Q
	172→132	−0.14±0.04	0.06±0.04	D[b]
	374→(172)→132	−0.09±0.06	−0.03±0.06	D
^{111}Ru	651→514	0.13±0.03	−0.20±0.31	Q
	514→358	0.12±0.02	−0.01±0.02	Q
	150→166	0.15±0.03	0.02±0.03	Q
	358→(76)→150	−0.07±0.02	−0.01±0.02	D
	150→(63)→104	−0.16±0.06	−0.06±0.06	D

[a]Quadrupole.
[b]Dipole.

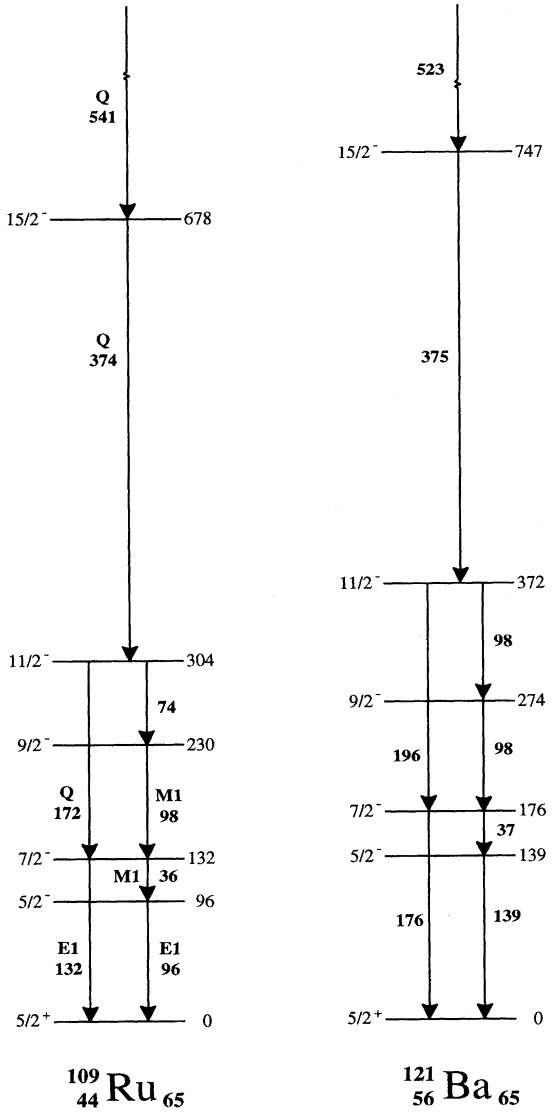

FIG. 7. Negative-parity level schemes of ^{109}Ru and ^{121}Ba. Spin and parity assignments for ^{109}Ru are based upon the indicated multipolarity or quadrupole-dipole character of transitions. The valence structure of the nuclide ^{121}Ba differs from ^{109}Ru only in that six protons are either hole or particle in character relative to the $Z=50$ shell.

observation of the $5/2^-$ state is a strong indication that all observed negative-parity states originate from the $5/2^-[532]$ Nilsson orbital.

The negative-parity low-energy level scheme of ^{109}Ru with its valence mirror nuclide ^{121}Ba [12] is plotted in Fig. 7. Both ^{109}Ru and ^{121}Ba have neutron number $N=65$. The only difference in proton structure is that six protons of ^{109}Ru are holes relative to the $Z=50$ shell, and six protons of ^{121}Ba are particle in nature relative to the $Z=50$ shell. The similarity in structure is remarkable, and tends to confirm again our spin assignments.

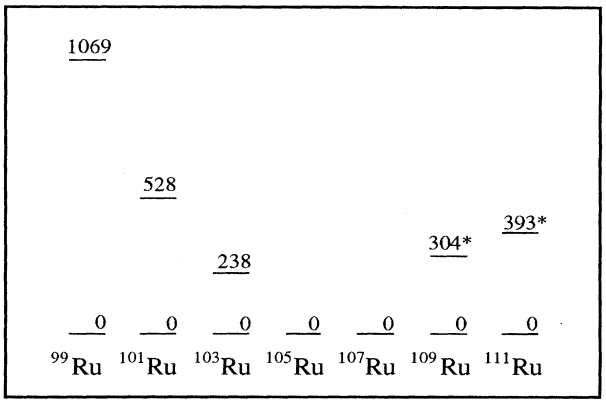

FIG. 8. Systematics of $11/2^-$ states in Ru isotopes. States with an asterisk are newly proposed.

C. Nuclide ^{111}Ru

The electric or magnetic nature of transitions in ^{111}Ru has not been determined. Angular correlation measurements did determine the quadrupole or dipole character of several transitions, and the results are recorded in Table I. Since the electric or magnetic character of the transitions has not been determined, and because the ground state spin of ^{111}Ru is unknown, we have not assigned spins and parities to the low-energy states in ^{111}Ru. The similarity between ^{109,111}Ru in the high-energy portion of the level schemes and the stretched quadrupole nature of γ-γ cascades suggest the assignment of $J^\pi=11/2^-$–$27/2^-$ for the high-energy states.

A plot of known $11/2^-$ states in the neutron-rich Ru nuclides appears as Fig. 8. The $11/2^-$ states of ^{109,111}Ru, marked with an asterisk, have also been plotted in Fig. 8. The rise in excitation energy past ^{107}Ru must be more subtle than a "midshell effect," because a neutron midshell occurs at $N=66$, not as $N=60$, as Fig. 8 seems to indicate. Quantitative calculations will be needed to explain this and the other interesting data about nuclei in the $A\sim110$ region. The following calculations are fairly qualitative, and were performed to exhibit the relative energies of states arising from the coupling of an $h_{11/2}$ neutron to a triaxial core.

VI. NEUTRON+TRIAXIAL CORE MODEL CALCULATION

Since the even-even nuclides ^{108,110}Ru seem to exhibit properties of triaxial nuclei, we decided to couple an $h_{11/2}$ neutron to their respective triaxial cores in order to generate a theoretical energy spectrum for the band of each of ^{109,111}Ru. The model and computer code (ASQROT) we used is that of Meyer-Ter-Vehn [13]. This particle-core model describes a quasiparticle whose configuration space is restricted to a single j shell. Since we assume the states of interest arise from a unique-parity orbit, a restriction to the $j=11/2$ shell should be a good approximation.

This model is somewhat simplistic in that the core is assumed rigid. Without modifications it is unable to predict that the energies of states with angular momentum less than $j=11/2$ can fall below the energy of the 11/2 state. Nevertheless, the model has only four parameters, and two parameters are easily determined from experimental data. The pa-

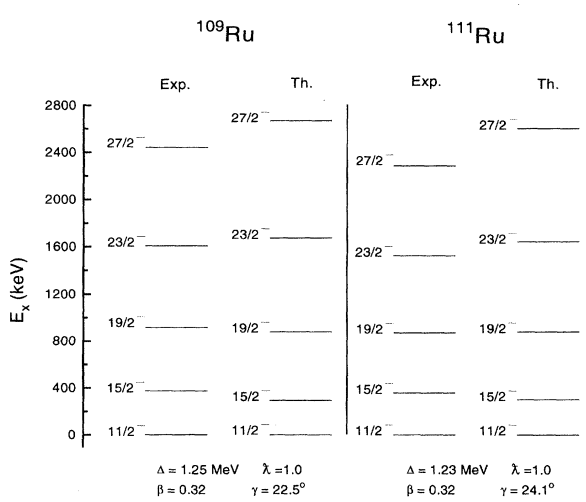

FIG. 9. Comparison between experimental and theoretical calculations of level schemes of ^{109,111}Ru. Theoretical level schemes have been calculated with the particle+triaxial core model, with parameters noted at the bottom of the figure.

rameters needed to describe the quasiparticle nature of the nucleon are the pairing energy Δ and the Fermi energy λ_f. The interaction of the quasiparticle with the rotating triaxial core is described with the deformation parameter β and asymmetry parameter γ.

The asymmetry parameter γ was obtained from the energy ratio of the first 2^+ state to the second 2^+ state in the core [13]. The first 2^+ excited states of adjacent even-even cores were used to deduce an initial value of $\beta=0.35$. However, this value is slightly larger than experimental measurements [14] of $\beta\sim0.30$, and so in the calculations we used a value of $\beta=0.32$. This value of β also improved the fit of the theoretical energy of the $15/2^-$ states with the experimental values. The pairing energy was chosen as $\Delta=135/A$. In the computer code we used, the Fermi energy λ_F is scaled relative to the splitting of the lowest two single-particle energies that result from diagonalizing the single-particle part of the nuclear Hamiltonian with the BCS quasiparticle transformation. The scaled parameter is denoted by the symbol χ_F:

$$\chi_F=(\lambda_f-\varepsilon_1)/(\varepsilon_2-\varepsilon_1). \quad (2)$$

The results of our calculations and a comparison with the experimental data appear in Fig. 9. In particle-core coupling calculations, there are always several final states with a given total angular momentum. Naturally, we chose the least energetic one for each spin. The general agreement between theoretical and experimental level schemes is good. We see that the model slightly underpredicts the energy of the $15/2^-$ states, and the energies of the $27/2^-$ states are overpredicted by $\sim$300 keV. The excessively high energy for the high-spin states is a well-known phenomenon [15] whose origin lies in neglecting the softness of the core.

It should be noted that the calculations presented in Fig. 9 assume prolate deformed cores. As energy spectra of the even-even core nuclei are symmetric about $\gamma=30°$, this model cannot distinguish between prolate and oblate shapes. Therefore, one has to perform calculations for both shapes. Calculations based on oblate deformation (not shown in Fig. 9) were found to be in significant disagreement with experimental values.

VII. CONCLUSION

Experimental results and arguments for a band of states built on the $\nu h_{11/2}$ orbital have been presented for the neutron-rich nuclides ^{109,111}Ru. A cascade of transitions of smoothly increasing energy in each of ^{109,111}Ru was substantiated with single and double gated spectra from ^{252}Cf SF data. It was noted that other odd-A nuclei with $A\sim110$ exhibit yrast bands built on the $h_{11/2}$ orbital. Angular correlation measurements were capable of illustrating the $\Delta J=2$ character of the transitions in the band. Spin assignments for ^{109}Ru were based upon AC and conversion electron studies. Finally, theoretical level schemes were calculated with a particle+triaxial core model, with values of the parameters used in the calculations constrained by experimental values. The general agreement between the theoretical and experimental level schemes is further evidence for a $\Delta J=2$ band of states built on the $\nu h_{11/2}$ orbital.

ACKNOWLEDGMENTS

We gratefully acknowledge the help of Michael Winston, a teacher in the 1994 INEL Summer Research Program. One participating high school student, Dean Murray, discovered new transitions in ^{111}Ru that were later incorporated in this article. Work at the INEL was supported by the U.S. Department of Energy through the LITCO LDRD Program under the DOE Field Office, Idaho Contract No. DE-AC07-76ID01570. Work at Vanderbilt and LBL was supported by the U.S. Department of Energy under Grants and Contracts DE-FG05-88ER40407 and DE-FG03-87ER40323, respectively.

[1] E. Cheifetz, R. C. Jared, S. G. Thompson, and J. B. Wilhelmy, Phys. Rev. Lett. **25**, 38 (1970).

[2] W. R. Phillips, R. V. F. Janssens, I. Ahmad, H. Emling, R. Holzmann, T. L. Khoo, and M. W. Drigert, Phys. Rev. Lett. **57**, 3257 (1986).

[3] K. Butler-Moore, J. H. Hamilton, A. V. Ramayya, X. Zhao, W. C. Ma, J. Kormicki, J. K. Deng, W. B. Gao, J. D. Cole, R. Aryaeinejad, I. Y. Lee, N. R. Johnson, F. K. McGowan, G. Ter-Akopian, and Y. Oganessian, J. Phys. G **19**, L121 (1993).

[4] R. Aryaeinejad, J. D. Cole, R. C. Greenwood, S. S. Harrill, N. P. Lohstreter, K. Butler-Moore, S. Zhu, J. H. Hamilton, A. V. Ramayya, X. Zhao, W.-C. Ma, J. Kormicki, J. K. Deng, W. B. Gao, I. Y. Lee, N. R. Johnson, F. K. McGowan, G. M. Ter-Akopian, and Yu. Ts. Oganessian, Phys. Rev. C **48**, 566 (1993).

[5] A. G. Smith, W. R. Phillips, J. L. Durell, W. Urban, B. J. Varley, C. J. Pearson, J. A. Shannon, I. Ahmad, C. J. Lister, L. R. Morss, K. L. Nash, C. W. Williams, M. Bentaleb, E. Lubkiewicz, and N. Schulz, Phys. Rev. Lett. **73**, 2540 (1994).

[6] J. A. Shannon, W. R. Phillips, J. L. Durell, B. J. Varley, W. Urban, C. J. Pearson, I. Admad, C. J. Lister, L. R. Morss, K. L. Nash, C. W. Williams, N. Schulz, E. Lubkiewicz, and M. Bentaleb, Phys. Lett. B **336**, 136 (1994).

[7] H. Penttilä, Ph.D. thesis, University of Jyväskyläa, Finland, 1992.

[8] F. F. Hopkins, J. R. White, C. F. Moore, and P. Richard, Phys. Rev. C **8**, 380 (1973).

[9] J. Äystö, P. P. Jauho, Z. Janas, A. Jokinen, J. M. Parmonen, H. Penttilä, P. Taskinen, R. Béraud, R. Duffait, A. Emsallem, J. Meyer, M. Meyer, N. Redon, M. E. Leino, K. Eskola, and P. Dendooven, Nucl. Phys. **A515**, 365 (1990).

[10] C. M. Lederer and V.S. Shirley, *Table of Isotopes*, 7th ed. (John Wiley&Sons, New York, 1978).

[11] S. Juutinen, P. Šimeček, C. Fahlander, R. Julin, J. Kumpulainen, A. Lampinen, T. Lönnroth, A. Maj, S. Mitarai, D. Müller, J. Nyberg, M. Piiparinen, M. Sugawara, I. Thorslund, S. Törmänen, and A. Virtanen, Nucl. Phys. **A577**, 727 (1994).

[12] B. Cederwall, A. Johnson, R. Wyss, C. G. Lindén, S. Mitarai, J. Mukai, B. Fant, S. Juutinen, P. Ahonen, and J. Nyberg, Nucl. Phys. **A529**, 410 (1991).

[13] J. Meyer-Ter-Vehn, Nucl. Phys. **A249**, 111 (1975).

[14] G. Mamane, E. Cheifetz, E. Dafni, A. Zemel, and J. B. Wilhelmy, Nucl. Phys. **A454**, 213 (1986).

[15] H. Toki and A. Faessler, Nucl. Phys. **A253**, 231 (1975).